ESR of Mn^{+2} in calcium fluorophosphate. II. Modified Ca(II) sites

R. W. Warren and R. Mazelsky
Westinghouse Research Laboratories, Pittsburgh, Pennsylvania 15235
(Received 30 June 1972)

Crystals of calcium fluorophosphate containing manganese were grown under a variety of conditions with large deviations from stoichiometry. ESR measurements show the presence of two new centers both of which involve manganese bound to intrinsic oxygen-fluorine-vacancy defects. The dependence of their concentrations upon stoichiometry, manganese concentration, and thermal treatment is discussed. Models for these centers are proposed.

INTRODUCTION

Calcium fluorophosphate, often called FAP, has an extensive record[1-9] of optical and ESR measurements which have been performed on the impurities and defects which it sometimes contains. Information on these defects has also been obtained from measurements of the diffusion processes which occur at high temperatures.[10] These efforts have been immeasurably advanced by the ability to grow large single crystals[11-13] and to vary at will their stoichiometry and the content of various impurities. The symmetry and structure of FAP have been determined in considerable detail.[14] It crystallizes in the hexagonal apatite lattice with a unit cell composed of $Ca_{10}(PO_4)_6F_2$. There are two inequivalent calcium sites in the unit cell—one, with threefold rotational symmetry, called the Ca(I) site and the other, with reflection symmetry in the plane perpendicular to the threefold axis, called the Ca(II) site. ESR measurements show that when Mn is dissolved in apatite it substitutes for Ca at both of these sites.[8] ESR measurements also commonly show the presence of Mn in other unknown sites of lower symmetry.[3] The purpose of this paper is to present models for two of the most common "unknown" centers and to describe their formation. The models are based upon the symmetry and other features of their ESR spectra, the properties of the intrinsic oxygen-fluorine-vacancy defects in FAP, and the way in which the concentration of Mn at these "unknown" sites depends upon the stoichiometry of the melts from which the samples were grown.

EXPERIMENTAL TECHNIQUE

Crystals of FAP were grown from a melt composed of the raw materials $CaHPO_4$, CaF_2, and $CaCO_3$ in the ratio 6:1:3. Crystals were also grown from melts deviating substantially from this stoichiometric ratio. The CaF_2 content was varied from 0.6 to 3.0 times the stoichiometric value and the $CaCO_3$ content was varied from 0.8 to 1.2 times this value. Mn was added to the melt as $MnCO_3$ replacing an equal amount of $CaCO_3$. Further details of the growth process were described by Mazelsky, Hopkins, and Kramer.[13]

The crystals grown were examined using chemical analyses, x-ray-lattice parameter measurements, and density determinations. The results are all consistent with the existence of a finite width in the solidus phase field.[13] No crystals were found with a $CaF_2/Ca_9(PO_4)_6$ ratio greater than 1.00 even when there was a large excess of CaF_2 in the melt. However, at $CaF_2/Ca_9(PO_4)_6 = 0.6$ in the melt, deficiencies of CaF_2 in the order of 10% were observed in the crystals grown. Compositions approaching stoichiometry were obtained in crystals only when the melt composition was $CaF_2/Ca_9(PO_4)_6 \geq 1.4$.

Samples were prepared from the crystalline boules by cutting and polishing operations such that the final specimens were usually in the form of thin slabs with the crystalline c axis parallel to the surface of the slab. This technique resulted in samples whose shape was suitable for ESR and optical measurements. Optical measurements have been made on these crystals and reported by Ryan *et al.*[15] ESR measurements have previously been made on some of these crystals to identify and characterize the Mn(I) and Mn(II) centers.[8] The ESR techniques used in this present work are identical to those used earlier and are in most respects quite conventional.

RESULTS

ESR spectra

Figure 1 shows the ESR spectrum for a FAP crystal grown from a melt containing 0.1% Mn and a threefold excess of CaF_2. The strong lines are due to Mn(I), i.e., Mn substituted at the Ca(I) site. Figure 2 shows an enlargement of the central part of this spectrum showing the doublets due to Mn(II), i.e., Mn substituted at the Ca(II) site. The measurements were made at 77 K with the magnetic field parallel to the c axis of the crystal. These spectra are very sharp and their interpretation in

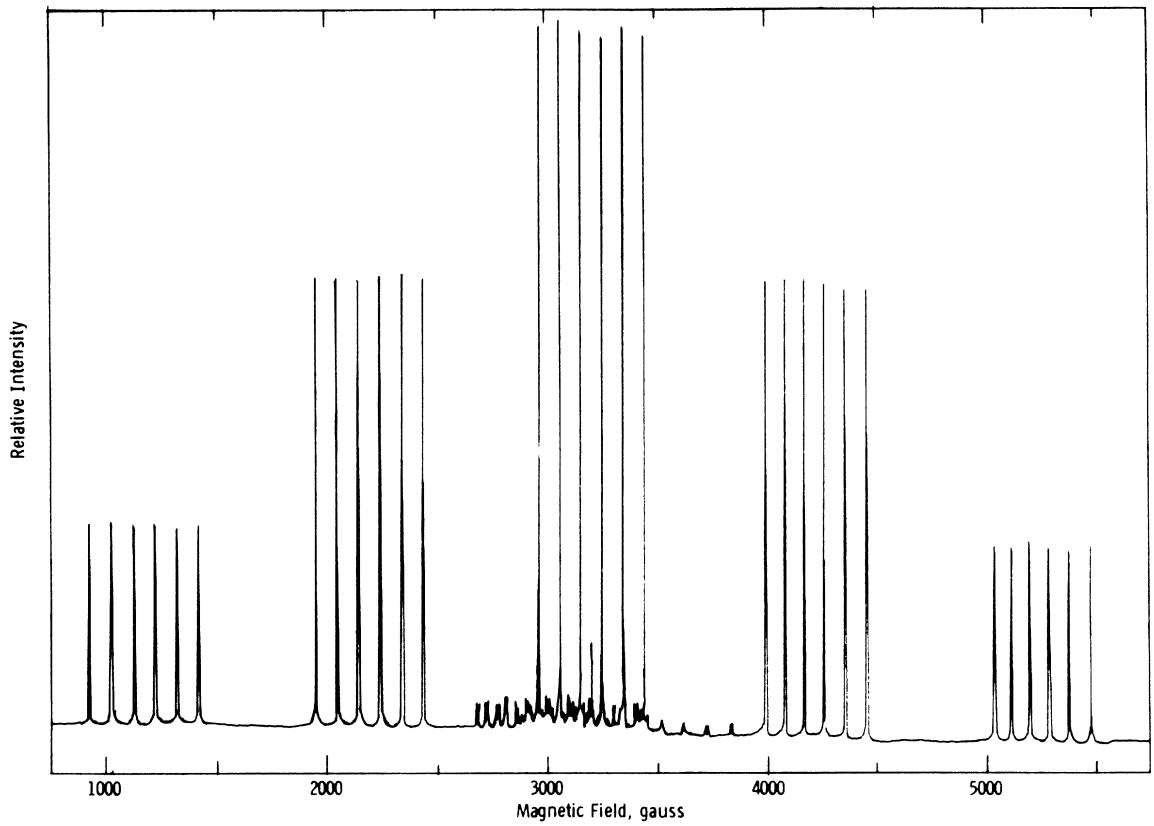

FIG. 1. ESR signal with H parallel to c for a sample grown with an excess of CaF_2.

terms of Mn ions substituted at the Ca(I) and Ca(II) sites is unequivocal.[8] If the magnetic field is rotated more than about 10° from the direction shown, the spectra become much more complicated and difficult to interpret. This is for two reasons. First, because of its low symmetry Mn(II) has a complicated ESR pattern which is a composite of spectra contributed by three Mn(II) centers in equivalent but not identical sites. The patterns merge into one only when the field is parallel to the c direction. Secondly, when the field is parallel to the c axis it is oriented along a high-symmetry direction of both the Mn(I) and Mn(II) centers. When the field is 10° from this direction, forbidden transitions of several kinds occur with high probability. They contribute a host of strong new lines for each center, Mn(I) and Mn(II). These forbidden transitions have been discussed previously for

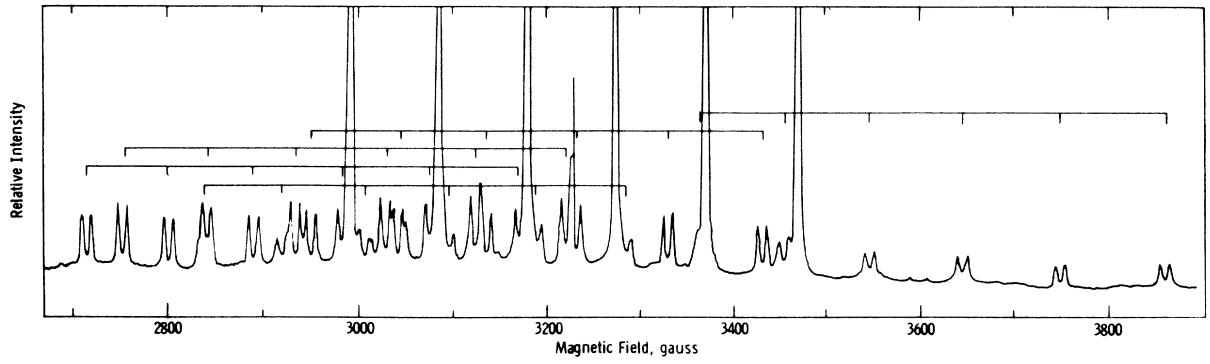

FIG. 2. Detail of the central part of Fig. 1 showing the spectrum due to the Mn(II) center.

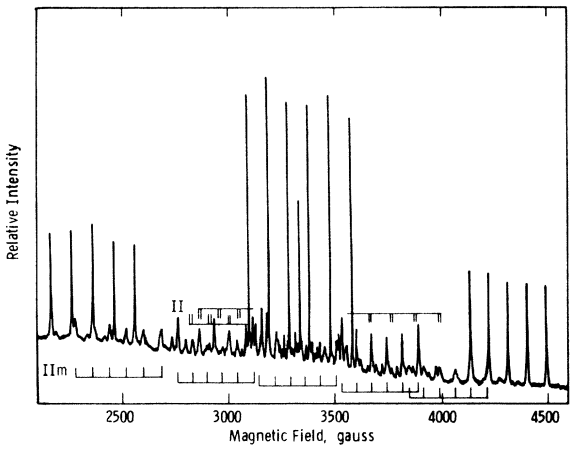

FIG. 3. ESR signal with H parallel to c for a sample grown from a stoichiometric melt. The lines due to the Mn(II) center and the positions at which the Mn(II) lines should appear are shown by flags.

Mn(I).[8]

Any center with a symmetry lower than Mn(II) will have an even more complicated spectrum, for there will then be six equivalent sites, each contributing its distinct spectrum. In addition, there is no orientation of the field which will make all of the equivalent spectra merge and at the same time be along a principal axis of all the centers so as to suppress the forbidden transitions. The centers we discuss below have this low symmetry and therefore display a complicated set of spectral lines.

Figure 3 shows the ESR spectrum of a FAP crystal grown from a melt containing 0.1% Mn. The melt was stoichiometric. The magnetic field is parallel to the c axis as in Figs. 1 and 2. The major sharp lines are due to Mn(I). The normal positions of Mn(II) lines are shown with flags labeled II. These lines are absent or very weak. A series of new broader Mn lines are apparent which we have labeled IIm. Their strength is comparable with the Mn(I) set. The central set of Mn(IIm) lines cannot be seen, for it is buried in the center of the spectrum. The labeled Mn(IIm) spectrum is not very sharp and some of the unlabeled lines seen in Fig. 3 are also caused by Mn(IIm). This complexity occurs because the principal axes of the Mn(IIm) center do not include the crystalline c axis so that forbidden lines are prominent.

From the size of the forbidden lines, one can estimate how far from the c axis a principal axis of this center must be. One finds roughly 20°. If this angle were much larger, the forbidden transitions would be so important that the spectrum would be split up and each line reduced in strength until the pattern would be totally obscured by the stronger Mn(I) spectrum. This point will be emphasized later in these discussions.

Spin Hamiltonian

Spectra of the Mn(IIm) center were carefully measured for various angles of the magnetic field relative to the c axis. The results were fit with the usual spin Hamiltonian[8] containing the parameters g, $D/g\mu_B$, $E/g\mu_B$, $A/g\mu_B$, and the angles describing the orientation of the principal axes of the Mn(IIm) center relative to the crystalline axes. The values found for these parameters are given in Table I. Also given are the parameters found for the Mn(II) center by Warren[8] and those for the Mn(IImm) centers to be discussed below.

The experimental data which provided the parameters for the Mn(IIm) and Mn(IImm) centers were meager. This is because the spectra of these centers were partially obscured by other stronger overlapping resonances. Because of this, only the outer 5/2–3/2 transitions could normally be observed. The procedure used to obtain the data needed for Table I was as follows. A resonance due to a given center was observed as the crystal was rotated relative to the magnetic field. The rotation was continued until an absolute extremum was found for the resonance line being followed. The value of this extremum, the angles at which it occurred, and the hyperfine splitting were recorded. A search was made to see if the other fine-structure resonances which occur at this angle could also be seen. If so, they too were recorded. There is, in general, one other direction in the crystal at which another extremum occurs for this center. This direction was found and the same kind of data was again taken. The direction which gave the larger extremum is called the z direction and the other the y direction. This choice for the

TABLE I. Parameters which enter the spin Hamiltonian for the Mn(II), Mn(IIm), and Mn(IImm) centers.

Mn Center	g	$D/g\mu_B$ (G)	$E/g\mu_B$ (G)	$A/g\mu_B$ (G)	θ_{cz}	θ_{cy}	ϕ_{az}
II	2.00	−504	−114	−96	90°	90°	0°±2°
IIm	2.00	−315±10	−90±10	−72±3	80°±2°	35°±2°	4.5°±2°
IImm	2.00	665±20	210±20	−82±3	86°±2°	12°±2°	2.5°±2°

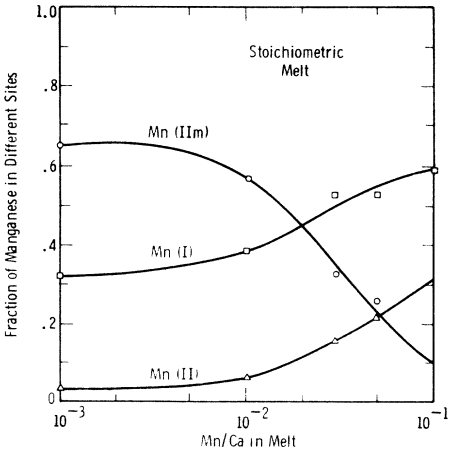

FIG. 4. Fraction of Mn(II), and Mn(IIm) in crystals of FAP vs the ratio of Mn/Ca in the melt for a stoichiometric melt.

axes leads to values for D and E which have the same sign. θ_{cz} given in Table I is the polar angle which was measured between the crystalline c direction and the z direction. θ_{cy} is the corresponding polar angle for the y direction. ϕ_{az} is the azimuthal angle between the z axis and the crystalline a axis. The a axis, a translation vector of the unit cell, is approximately the same as the direction defined by the Ca(II)–fluorine-ion bond in FAP.[8] A, the hyperfine parameter is isotropic within the precision of our measurements. The sign of A was assumed to be negative. The sign of D was then determined by comparing the hyperfine splitting among the fine-structure components as discussed by Low.[16]

Now there are two kinds of information shown in Table I which are derived from the measurements—that which is directly measured like θ_{cz} and θ_{cy} (or measured with respect to a reference angle like ϕ_{az}) and that which is determined by fitting measured data to the spin Hamiltonian like $D/g\mu_B$, $E/g\mu_B$, $A/g\mu_B$ and g. For the purposes of this experiment, the former are important and were measured with care and a reasonable precision. The latter are much less important. That is fortunate, for the fitting operation is difficult. The values of g, $A/g\mu_B$, $D/g\mu_B$, and $E/g\mu_B$ given in the table are only approximate. They result from a fit of the data to Low's second-order approximate solution to the spin Hamiltonian.[17] Earlier work with Mn(II) using both Low's formula and an exact diagonalization, shows that such a fit using Low's formula can be off by 10% or so. The major reason for the discrepancy is that a second-order approximation is not good enough when D and E are so large. To achieve a good fit, crystal-field terms higher than second order should also be considered.

Another comment on Table I is that ϕ_{ay} is not given. The three angles, θ_{cz}, θ_{cy}, and ϕ_{az}, are sufficient to define the direction of the Z axis in the crystal, but leave a twofold uncertainty in the value of ϕ_{ay} and thus the Y direction. For the Mn(IIm) center, for instance, this angle must be either $-100°$ or $+109°$. Since there appears to be no reason to determine this angle for the purposes of this paper, and because it is difficult to do so experimentally owing to the confusion resulting from so many overlapping spectra, we do not present values of ϕ_{ay} in Table I.

Dependence on stoichiometry and Mn concentration

The Mn(I), Mn(II), and Mn(IIm) lines dominate the spectra in all of the samples of FAP that were examined. ESR spectra due to other kinds of Mn or to other defects were observed, but their concentrations were always low.

The areas under the Mn(I), Mn(II), and Mn(IIm) spectra were measured and the fraction of the total contributed by each center was calculated. This fraction is plotted in Fig. 4 versus the ratio of Mn : Ca in the melt for a stoichiometric melt. The same measurements were performed for samples grown from a melt containing a threefold excess of CaF_2. These measurements are shown in Fig. 5. The upper limit to the Mn concentration in the melt is about 10%, for above this concentration, the individual lines in the ESR spectra become so broad that the overlapping spectra of Mn(I), Mn(II), and Mn(IIm) become unresolvable. The lower limit to the Mn concentration is about 10^{-3} for below this limit signal-to-noise problems become troublesome, and, in addition, nothing new seems to be happening.

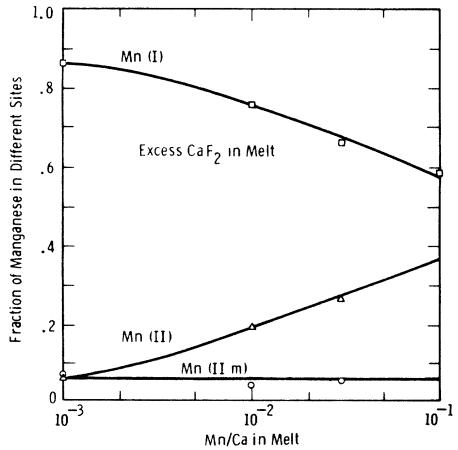

FIG. 5. Fraction of Mn(I), Mn(II), and Mn(IIm) in crystals of FAP vs the ratio of Mn/Ca in the melt for a melt containing a threefold excess of CaF_2.

An interesting observation, made especially from Fig. 5, is that the distribution coefficient between the Mn(I) and Mn(II) sites is not constant, but steadily changes as the Mn concentration increases. This has been discussed by Ryan *et al.*[15] He explains this change upon a steady reduction in the lattice dimensions of FAP, caused by the presence of increasing amounts of Mn ions, which makes substitution at the Mn(II) site more favorable.

It is also clear upon comparing the data of Figs. 4 and 5 that excess CaF_2 in the melt has not altered the distribution coefficient between Mn(I) and Mn(II) significantly, but it has been very effective in eliminating the Mn(IIm) center, especially at low Mn concentrations. The behavior of the curves in Figs. 4 and 5 suggests a coupling of Mn and another defect which is only present in the stoichiometric crystal. We propose the following model to explain the formation of the Mn(IIm) centers and the importance of stoichiometry:

(i) There is an unidentified defect (called X) which is present in crystals grown from stoichiometric melts but not CaF_2-excess melts. It has a concentration of about 10^{18} cm^{-3}.

(ii) When Mn is added to a melt containing X, the Mn is incorporated in the normal way in the crystal as it grows. Upon cooling, the Mn ions tend to couple to the X centers which are also present in the crystal to form the complex Mn(IIm). The complexing does not normally consume all of the X and Mn, but leaves some in the free state.

(iii) When enough Mn ions are added to the crystal, nearly all of the X centers are consumed and any additional Mn ions sit at the normal Mn(I) and Mn(II) sites as in CaF_2-excess crystals.

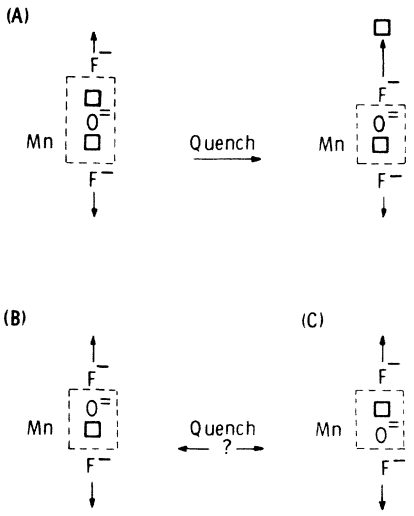

FIG. 6. Models proposed for the Mn(IIm) center, A; the Mn(IImm) center, B; and another hypothetical center C.

Other recent work on FAP lends strong support to this model. Warren[18] has shown that stoichiometric FAP contains a defect whose concentration is about 2×10^{18} cm^{-3} and whose properties exactly match those of the X center described above. In particular, its concentration depends upon stoichiometry in the required way and it is "consumed" if a high-enough concentration of Mn is also present. The optical properties of this defect have been examined by Ryan *et al.*[15] It has been identified by Warren[18] as $(VOV)^+$, i.e., a complex composed of two fluorine vacancies, V, and one oxygen ion, O, substituted for fluorine. The positive sign signifies that this complex has a net positive charge relative to the three fluorine ions it replaces. In addition, Warren finds that FAP contains a large concentration of $(OV)^0$ and probably $(V)^+$ and $(O)^-$, i.e., defects composed of other clusters of fluorine vacancies and oxygen or these separate defects. All of these defects have properties similar to the $(VOV)^+$ center and thus might also be the X center.

Possible models for Mn(IIm)

We have shown that the Mn(IIm) center involves Mn and the $(VOV)^+$ complex or some other center like it composed of $(O)^-$ and $(V)^+$ defects on the fluorine chain in FAP. The only reasonable position for Mn is the Ca(I) or Ca(II) site. Because of the large differences between the spectra of Mn(IIm) and Mn(I) or Mn(II), the Mn ion in Mn(IIm) must be strongly perturbed by the presence of $(VOV)^+$. We can conclude from this that the Mn ion must be very near to $(VOV)^+$ and is probably at the nearest Ca(II) site. The only reasonable alternative is the nearest Ca(I) site, but this site is already spaced so far from the fluorine chain that an ESR spectrum of such a complex should be only slightly different from that of an isolated Mn(I) ion. We, in fact, do observe just such a spectrum and tentatively assign it to this complex of Mn on the Ca(I) site coupled to a distant $(VOV)^+$ complex. This spectrum is always quite weak and will not be discussed further here.

Further evidence for a model with Mn at the nearest Ca(II) site is the value of θ_{cz} and ϕ_{az} found for this center. These values are very close to those of the Mn(II) center showing that the major axes of the ellipsoids describing the electric field for Mn(IIm) and Mn(II) are oriented in nearly the same direction and suggesting that these centers are closely related.

Having restricted the Mn ion to the Ca(II) site and the X center to one of those complexes of $(O)^-$ and $(V)^+$ for which there is experimental evidence, i.e., $(V)^+$, $(O)^-$, $(OV)^0$, and $(VOV)^+$, we find that

there are only three combinations of Mn and these complexes which can satisfy the observed ESR results. These are combinations which lack reflection symmetry in the plane perpendicular to the c axis and have no neighboring fluorine ion to give Mn a large (i.e., >1 G) superhyperfine splitting. The three possibilities are shown in Fig. 6 and are labeled A, B, and C. In this figure, the crystalline c axis is vertical. The oxygen–fluorine-vacancy complexes are substituted in the chain of fluorine ions that extends throughout the crystal in the c direction. The Mn ion is substituted on a Ca(II) site next to this fluorine chain. Model A, i.e., Mn near $(VOV)^+$, is the one that we propose for Mn(IIm). The reasons for picking this rather than one of the other two models will be discussed below.

Quenching behavior

In the work described above[18] on the properties of the X center in "pure" FAP, quenching experiments were performed. These showed that $(VOV)^+$ was destroyed thermally at around 600 °C and that a rapid quench to room temperature could keep some of the decomposition products [probably $(OV)^0$ and $(V)^+$] from recombining for periods of many hours.

We checked to see whether this same type of quench would modify the Mn(IIm) center. The sample whose spectra is shown in Fig. 3, was heated to 600 °C for 1 h and then quenched in cold water. It was then mounted in the ESR apparatus and cooled to 77 K. The time the sample was held at room temperature, before cooling to 77 K, was about 30 min. In this time, the decomposition products of $(VOV)^+$ would have recombined to the extent of about 50%.[18] Figure 7 shows the ESR measurements made on this quenched sample. From a comparison of Figs. 3 and 7, one can see that the quench has reduced the concentration of Mn(IIm) by a factor of about 2 or 3 while the Mn(I) and probably the Mn(II) spectra have changed only slightly, not enough to account for the drop in the Mn(IIm) spectra.

These results can be explained by the process shown diagrammatically at the top of Fig. 6. The X center near the Mn(II) center had dissociated, losing one vacancy, and a new low-symmetry Mn center has been created. This new center should be paramagnetic, but it cannot be detected in the ESR spectra of Fig. 7. It was eventually found after a careful search at different magnetic fields and crystal orientations. The data obtained, as for Mn(IIm), are quite fragmentary. The parameters found for this center, hereafter called Mn(IImm), are given in Table I. The values of D and E are very large. Because of this, the forbidden transitions are strong and very numerous and the overall spectra is very complex, composed of many weak overlapping lines which are difficult to resolve. This explains why no evidence of Mn(IImm) could be seen in Fig. 4 or 5. The important features of this center are that it, like Mn(IIm), lacks reflection symmetry and lacks a neighboring fluorine ion. It has θ_{cz} and ϕ_{az} values very close to that of the Mn(II) and Mn(IIm) centers. This suggests that all three centers are related.

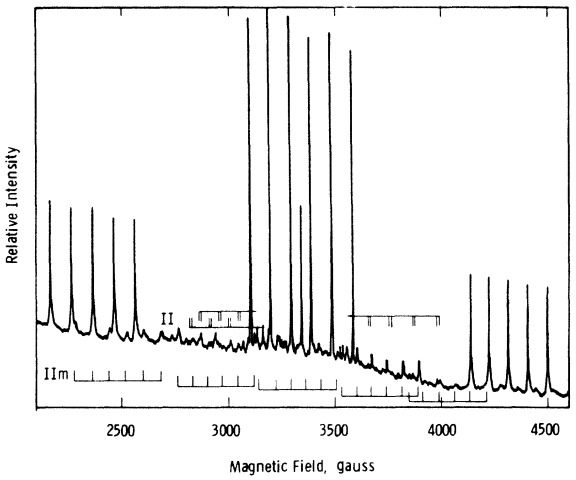

FIG. 7. ESR spectra with H parallel to c for the stoichiometric sample shown in Fig. 3 after it is heated to 600 °C and quenched.

We have proposed that Mn(IIm) is the complex called A in Fig. 6 and that heating and quenching converts it to Mn(IImm), the complex called B in Fig. 6. Alternative models for the Mn(IIm) and Mn(IImm) centers and the effect of quenching are possible. The most reasonable of these is shown on the bottom of Fig. 6. In this case, the quench does not free a vacancy from $(VOV)^+$ but instead inverts the $(OV)^0$ defect near the Mn ion. The strongest reason for preferring the top model is that the quenching process occurs at a temperature very similar to that of the free $(VOV)^+$ center, suggesting that Mn(IIm) involves this defect. Another reason involves the variations observed in the hyperfine parameter A between the Mn(II), Mn(IIm), and Mn(IImm) centers. If Mn is near a negative-ion vacancy, the Mn electrons are less tightly bound to it and leak over somewhat into the vacancy. This reduces the magnitude of A. Among the complexes shown in Fig. 6, this effect should cause A to decrease from its value in Mn(II) in the order model C, model B, and model A. If, as we propose, the sequence at the top of Fig. 6 occurs upon quenching, the Mn(IIm) center, model A, should show a smaller value for A than does the Mn(IImm) center, model B, and both values should be small-

er than the value for Mn(II). This prediction is in agreement with the measurements.

CONCLUSIONS

We propose that Mn ions which are added to FAP crystals containing $(VOV)^+$ defects are attracted and bound to these defects making a new complex called the Mn(II*m*) center. ESR spectra of this center have been observed and the important parameters entering the spin Hamiltonian have been evaluated for it. The mutual "gettering" action of the $(VOV)^+$ defect and the Mn ion continues as the Mn concentration is increased until the $(VOV)^+$ defects are all bound. Further Mn additions are then distributed on the Ca(I) and Ca(II) sites in a ratio similar to that found in crystals specially grown to have very few $(VOV)^+$ centers. When quenched from 600 °C to room temperature, Mn(II*m*) centers decompose, losing a vacancy, and become a new center called Mn(II*mm*). Annealing restores the Mn(II*m*) center. ESR spectra of the Mn(II*mm*) center have also been observed and its important parameters evaluated. Detailed models of the Mn(II*m*) and Mn(II*mm*) centers have been proposed.

ACKNOWLEDGMENTS

We gratefully acknowledge helpful discussions with F. M. Ryan concerning the optical properties of FAP and the experimental assistance of J. R. Sutter.

[1]P. D. Johnson, J. Appl. Phys. 32, 127 (1961).
[2]P. Kasai, J. Phys. Chem. 66, 674 (1962).
[3]Y. Ohkubo and H. Mizuno, in International Conference on Luminescence, Budapest, 1966 (unpublished), p. 6; Y. Ohkubo, J. Phys. Soc. Jap. 18, 916 (1963).
[4]S. P. Burley, Aust. J. Phys. 17, 537 (1964).
[5]R. K. Swank, Phys. Rev. 135, A266 (1964).
[6]W. W. Piper, L. C. Kravitz, and R. K. Swank, Phys. Rev. 138, A1802 (1965).
[7]J. S. Prener, W. W. Piper, and R. M. Chrenko, Phys. Chem. Solids 30, 1465 (1969).
[8]R. W. Warren, Phys. Rev. B 2, 4383 (1970).
[9]F. M. Ryan, R. C. Ohlmann, J. Murphy, R. Mazelsky, G. R. Wagner, and R. W. Warren, Phys. Rev. B 2, 2341 (1970).
[10]D. Den Hartog, D. O. Welch, and B. S. H. Royce, Phys. Status Solidi B 53, 201 (1972); D. O. Welch and B. S. H. Royce, Phys. Status Solidi B 57, 193 (1973).
[11]P. D. Johnson, J. Electrochem. Soc. 108, 159 (1961).
[12]J. S. Prener, J. Electrochem. Soc. 114, 77 (1967).
[13]R. Mazelsky, R. H. Hopkins, and W. E. Kramer, J. Cryst. Growth 7, 260 (1968).
[14]R. W. G. Wyckoff, *Crystal Structures*, 2nd ed. (Wiley, New York, 1965), Vol. III, p. 228.
[15]F. M. Ryan, R. C. Ohlmann, J. Murphy, R. Mazelsky, G. R. Wagner, and R. W. Warren, Phys. Rev. B 2, 2341 (1970).
[16]William Low, *Parametic Resonance in Solids* (Academic, New York and London, 1960), p. 71.
[17]William Low, Ref. 16, p. 57. The formula as shown contains numerical errors. A corrected form may be found in Ref. 2.
[18]R. W. Warren, Phys. Rev. B 6, 4679 (1972).